

Eclipse on the Coral Sea: Cycle 24 Ascending

Editors P. S. Cally, R. Erdélyi, A. A. Norton

Journal of Physics Conference Series

Ellerman bombs: fallacies, fads, usage

Robert J. Rutten^{1,2}, Gregal J. M. Vissers², Luc H. M. Rouppe van der Voort², Peter Sütterlin³ and Nikola Vitas⁴

¹ Lingezicht Astrophysics, 't Oosteneind 9, 4158 CA Deil, The Netherlands

² Institute of Theoretical Astrophysics, University of Oslo, P.O. Box 1029, Blindern, N-0315 Oslo, Norway

³ Institute for Solar Physics, Albanova University Center, SE-106 91 Stockholm, Sweden

⁴ Instituto de Astrofísica de Canarias, C/ Via Lactea S/N, E-38200 La Laguna, Tenerife, Spain

E-mail: R.J.Rutten@uu.nl

Abstract. Ellerman bombs are short-lived brightenings of the outer wings of $H\alpha$ that occur in active regions with much flux emergence. We point out fads and fallacies in the extensive Ellerman bomb literature¹, discuss their appearance in various spectral diagnostics, and advocate their use as indicators of field reconfiguration in active-region topography using AIA 1700 Å images.

1. Introduction

Ellerman [1] described “solar hydrogen bombs” in 1917 as intense brightenings of the extended wings of $H\alpha$, $H\beta$ and $H\gamma$, not visible in other lines and with the line cores unaffected. They last a few minutes and occur repetitively in active regions with much flux emergence, preferentially near and especially between penumbrae. These properties define the Ellerman bomb (EB) phenomenon. The subsequent EB literature cannot be fully reviewed here but we point out some fads and fallacies below. Bray and Loughhead [2] concluded in 1974 that “*extensive modern observations have added little to Ellerman’s original description*”. This lack of progress changed with high-resolution observing, first in the Flare Genesis flight [3] [4] [5] [6] [7] [8] and more recently with the Swedish 1-m Solar Telescope (SST) [9] [10].

2. Magnetic concentrations as pseudo Ellerman bombs

Figure 1 shows snapshots from 3-hour multi-wavelength Dutch Open Telescope (DOT) movies². The $H\alpha$ wing image in the lower-left panel shows many bright grains that in the movie adhere to Ellerman’s description: “*they seem to follow one another like the balls of a Roman candle*”. About half exceed the mean intensity by over 30%, a few are brighter than 54% (4σ) excess. Traditional EB threshold criteria might classify these as EBs. However, movie inspection including comparison with the parallel Ca II H and G-band movies shows that all the bright grains are simply “network bright points” marking strong-field magnetic concentrations (MCs). They are not EBs but “moving magnetic features” [12] [13] [14] [15] [16] [17]. Nor was there flux emergence in this region evident in SOHO/MDI magnetograms.

¹ Clicking on citation numbers should open the corresponding ADS abstract page in a browser.

² Links: four-panel movie, wing-only movie.

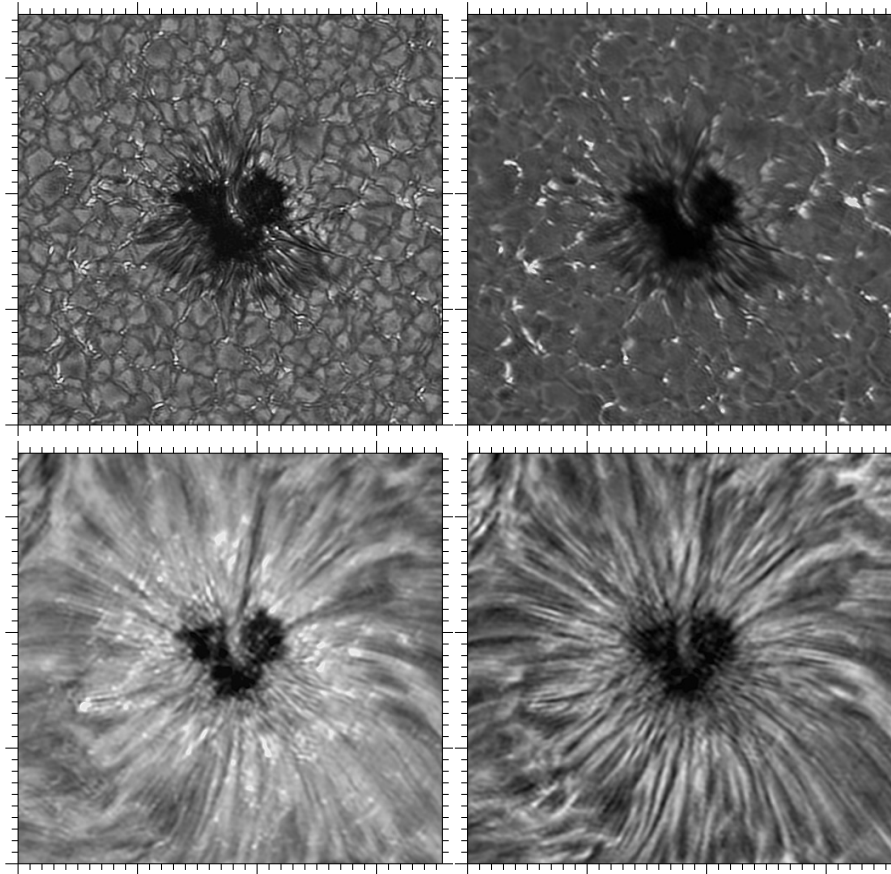


Figure 1. Simultaneous DOT images of the main spot of decaying AR10789 at view angle $\mu = 0.86$. Clockwise: G band; blue Ca II H wing at $\Delta\lambda = -2.35 \text{ \AA}$; sum of the H α wings at $\Delta\lambda = \pm 0.5 \text{ \AA}$; H α core. Tick marks: arcseconds.

MCs are bright in the continuum from hot-wall radiation [18]. The classic magnetostatic thin fluxtube/sheet paradigm [19] [20] [21] [22] [23] [24] [25] [26] explains their physics well and is well applicable [27], although actual MCs show complex morphology with rapid changes [28] [29]. Since MCs are small and reside in dark intergranular lanes, their continuum brightening is only seen at sub-arcsecond resolution [30]. MCs also appear as bright “line gaps” in the cores of neutral-metal lines due to ionization from evacuation, particularly in Mn I lines [31] [32] for which the contrast is not weakened by Dopplershifts in the surrounding granulation [11]. They also appear markedly bright in the outer wings of H α [33], at larger contrast than in other diagnostics including the G band [34]. For the G band the contrast enhancement comes from dissociation of the CH molecules producing this feature, for the H α wings from smaller collisional damping. Both result also from MC evacuation.

The H α core image in Fig. 1 shows the chromospheric fibril canopy that overlies and shields the deep photosphere imaged in the far H α wings. H α does not sample the intermediate layers (seen in Ca II H as shock-ridden clapotisphere [35]) due to its low-temperature opacity gap [36] [37] [38], so that at any wavelength its formation jumps between chromosphere and deep photosphere depending on the chromospheric fibril opacity. The $\Delta\lambda = \pm 0.5 \text{ \AA}$ sampling wavelength of Fig. 1 mixes deep-photosphere and upper-chromosphere brightness contributions, in this case MCs and superpenumbral fibrils. The fibrils look like the line-core ones but are thinner. The MCs show about the same morphology as in the Ca II-wing and G-band images

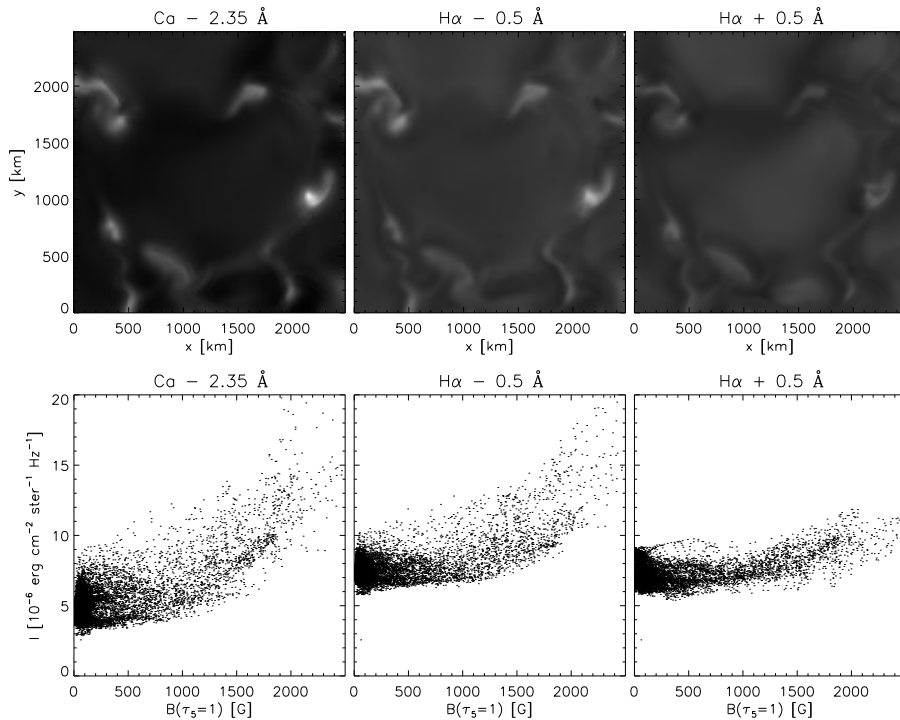


Figure 2. Synthesis of Ca II H wing and H α wing images for the numerical MHD simulation snapshot of [11]. The scatter plots show brightness against magnetic field strength per pixel. Downdrafts make some MCs, including the brightest, brighter in the blue H α wing.

because their brightness originates at about the same depth. The overlying fibrils block some MCs. Where they are sufficiently thin that the photospheric MC brightness shines through, they degrade the MC image sharpness. This defocus, compared to the sharp LTE-formed G-band and Ca II H-wing brightness features, results from ray spreading across the opacity gap and scattering through the effectively thin fibrils.

Note in the H α wing image that the shielding by overlying fibrils appears to be less for the MCs in the moat than for MCs further away. Larger transparency of superpenumbral fibrils may result from repetitive shock heating by running penumbral waves [39] [40], ionizing hydrogen too frequently to let it reach population equilibrium since hydrogen ionization/recombination balancing is exceptionally slow in cooling shock aftermaths due to the large $n=1-2$ Ly α transition [41] [42].

In the DOT movie some of the larger MCs do brighten momentarily, especially in the blue H α wing. Blue-wing brightening may result from MC downdrafts, as in the numerical simulation shown in Fig. 2. Downdrafts often occur in moat MCs that have opposite polarity to the sunspot [43]. MC downdrafts tend to produce shocks higher up [44] that are best seen in Na I D Dopplergrams [45]. Inspection of simultaneous H α and Na I D active-region Dopplergram sequences from the SST shows that such MC shock occurrence is often accompanied by H α blue-wing brightening.

MC brightening may also result from field concentration by bathtub vorticity in granular swirls [46]. Such brightening also reflects increasing hot-wall radiation, and must not be misinterpreted as MHD heating or reconnection [47]. However, swirl brightening seems a rare phenomenon. In the DOT data of Fig. 1 H α wing brightening shows no correlation with vorticity in the granular flows measured from the G-band movie. Rather, it happens in concert with

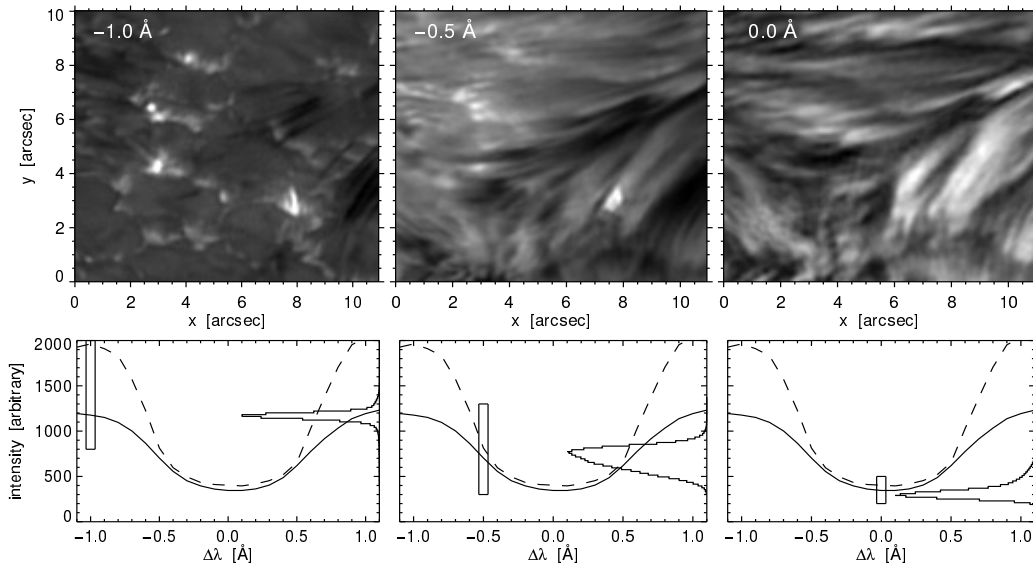


Figure 3. Upper row: SST EB images in H α at the specified wavelength separations from line center, taken from Fig. 1 of [9]. View angle $\mu = 0.67$ with the limb direction to the top. Lower row: H α profile (solid) averaged over the full 67×67 arcsec² field of view of the observations and H α profile (dashed) for a pixel in the EB at $(x, y) = (8.0, 2.5)$. The histograms show the normalized intensity occurrence distribution over the full observed field of view at each wavelength. The rectangle widths show the passband FWHM, the vertical extents the greyscale clipping of the corresponding images (each bytescaled for maximum contrast).

CaII H-wing brightenings that seem mostly due to episodes of magnetic patch [48] compression in the outward moat flow.

Upshot regarding EB fallacies: part of the EB literature (and the moustache literature, Severny’s [49] term for far-extended bright line wings) concerns MCs, not EBs. This is the case when dense network was not resolved, moustache brightening of the continuum and neutral-metal lines was observed, or when low H α -wing contrast thresholds were applied. In our opinion this warning should be heeded when reading [49] [50] [51] [52] [53] [54] [55] [56] [57] [58] [59] [60].

3. Ellerman bombs are not chromospheric

Figure 3 after Fig. 1 of [9] shows EBs at the unprecedented resolution of the SST. In this slanted limbward high-resolution view EBs appear in the outer H α wings as tiny bright upright flames that flicker rapidly while their footpoints travel along MC-filled network strands. The ensemble may be bright for many minutes but the subflames last only seconds. Inspection of the corresponding SST movies³ demonstrates this behavior irrevocably. The elongated shape was noted before in lower-resolution data [61] [4] [62], as was their intermittent substructure [63].

Figure 3 also demonstrates that EBs are purely photospheric phenomena. They are not seen at H α line center because the flames, even when tall (a few hundred to a thousand km [64] [61] [65]), do not break through the overlying dense canopy of chromospheric H α fibrils that always covers a growing active region. Comparison of the greyscale ranges (narrow rectangles in the lower panels of Fig. 3) shows that the EB wing emission is much brighter than the brightest line-core features. Some diffuse line-center brightening might again result from photospheric EB emission that passes through the opacity gap and scatters through the fibrils, but our SST

³ <http://iopscience.iop.org/0004-637X/736/1/71/fulltext>; one example.

movies suggest that such line-center brightening above EBs is uncommon. At $\Delta\lambda = -0.5$ Å the fibrils show the same morphology as at line center but they are less opaque and therefore brighter [38], except for blueshifted dark ones seen also at $\Delta\lambda = -1.0$ Å. At $\Delta\lambda = -0.5$ Å the EBs do shine through, again with loss of sharpness from scattering. Some MCs also shine through, but less brightly than in Fig. 1 because the bytescale now includes much brighter EBs and the H α fibril canopy is thicker in this flux-emergence region than around the little decaying spot of Fig. 1.

Thus, an EB top may reach higher than the 400–500 km nominal height of the temperature minimum in standard one-dimensional static-equilibrium models of the solar atmosphere [66] [67] [68] [69]. The onset of the actual solar outward temperature rise likely varies between 200 km in MCs and 2000 km in internetwork, varying temporally as well [42] [70], but in any case, the jet-like EB flame protrusions originate from the deep photosphere, in the network at the EB footpoint, and do not affect or poke through the overlying chromosphere defined [35] by the H α fibrils.

Apparent blue-brighter-than-red EB wing asymmetry [71] usually results from inverse Evershed flows [72] [73] [74] along the fibrils, the dark chromospheric line core shifting into the red-wing emission. Thus, asymmetries and wavelengths of EB emission peaks do not define Dopplershifts of the EB emitting material [59] [6] but are set by the absorbing overlying fibrils [75].

It has been suggested that EBs are accompanied by H α surges [76] [77] [78] [79] [80] [81]. However, the high-resolution SST data of [9] contained only two tentative cases. Our newer SST data sampled in Fig. 4 contain at most one questionable case [10]. An EB–surge connection is certainly not ubiquitous [4].

Upshot regarding EB fallacies: most EB papers err in describing the EB phenomenon as chromospheric. It is not. EBs have no systematic counterpart in the overlying chromosphere, transition region or corona. Dark chromospheric H α cores are not EB ingredients, nor are their Dopplershifts.

Comment regarding EB fads: EBs may combine strong downflows in the low photosphere [82] with outward flows higher up [81] [9]. Such bi-directional flows are reminiscent of “chromospheric anemone jets” seen in Hinode Ca II H data [83] [84] [85]. If such Ca II H jets actually are EBs, they are also confined to the photosphere. Just as for H α , not every bright Ca II H feature is necessarily chromospheric.

4. Ellerman bomb visibility

Even though they are photospheric, proper EBs (those that adhere to Ellerman’s description) do not show up in neutral-metal lines nor in the continuum. At sufficient angular resolution they do show continuum moustaches, G-band brightening [86], and narrow neutral-line gaps at their footpoint, sampling the MC from which they arise. Ellerman wrote: *“they frequently appear in the faculae so that their spectra are superposed on those of faculae, thus giving the appearance of great extension to the bright “bomb” band”* which wasn’t heeded in most pseudo-EB literature.

EB flames are also observable in Ca II 8542 Å, Ca II H&K, and in mid-UV continua [87] [4] [6] [88] [89] [62] [90] [91] [86] [10]. They are not identically the same in these different diagnostics, but they often show up at the same space-time locations. We illustrate this for the 1700 Å continuum in Fig. 4 by combining image cutouts from the new SST data of [10] with co-aligned image cutouts from SDO. Clearly, AIA’s 1700 Å shows the larger EBs also, at much lower resolution but with less interference by chromospheric fibrils. Since this continuum originates in the upper photosphere [67] [92], the bottom part of an H α EB is hidden in slanted 1700 Å viewing but this is not noticeable at AIA’s angular resolution.

AIA’s 1600 Å images (not shown) show the EBs too, at yet larger contrast, but these also show a few more extended and yet brighter transition-region transients for this area and period.

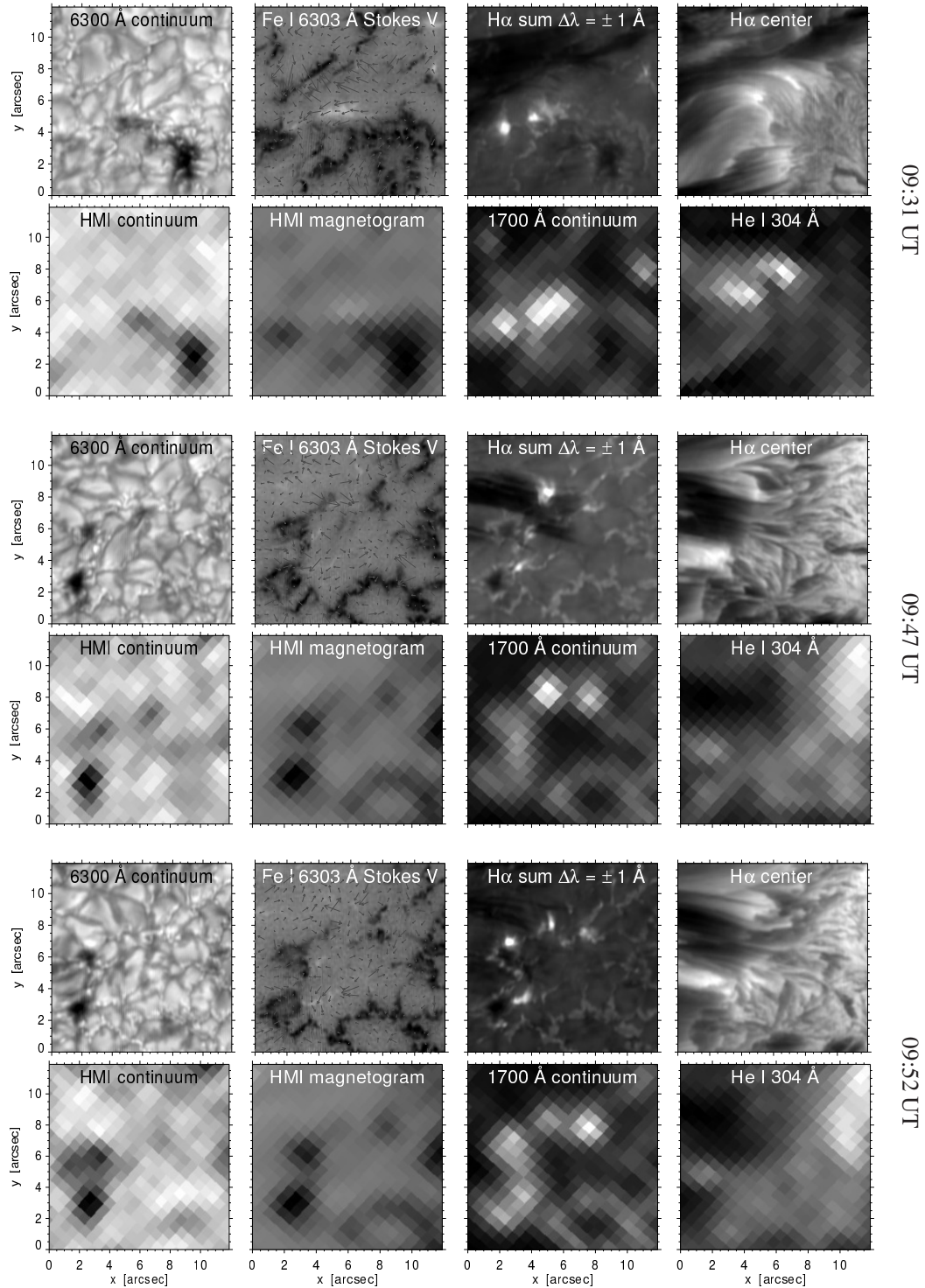


Figure 4. Two small-field cutouts of corresponding SST images (upper row of each set) and SDO images (lower rows) from the data of [10]. Magnification per pdf viewer is recommended for the SST images. View angle $\mu = 0.89$; the panel tops are in the limb direction. The third set shows the same cutout as the second, but five minutes later. Each panel is bytescaled independently. The arrows overlaid on the SST magnetograms show surface flows measured from the continuum sequence by correlation tracking.

They have short-loop morphology and correspond to bright patches in $H\alpha$ line-center, are also seen in $\text{He I } 304 \text{ \AA}$, and sometimes in $\text{Fe IX-X } 171 \text{ \AA}$. These loop-like bright transients appear unrelated to underlying EBs. We attribute their visibility in the 1600 \AA images to the CIV lines in this passband and tentatively identify them as upper-atmosphere transients such as small flaring arch filaments and microflares visible in transition-region diagnostics and $H\alpha$ line center. The $\text{He I } 304 \text{ \AA}$ images in Fig. 4 indeed mimic the $H\alpha$ line-center morphology which appears indifferent to EBs underneath.

It is illustrative and recommended to play and blink SDO 1700 \AA , 1600 \AA , and $\text{He I } 304 \text{ \AA}$ movies of a very active region with much flux emergence, for example AR 11654 on January 10, 2013 and the following days when it was crackling with short-lived brightenings in these diagnostics. The plethora of transient brightness features in 1600 \AA are the sum of different sorts, respectively seen in 1700 \AA and in $\text{He I } 304 \text{ \AA}$. Very short-lived, pointlike 1700 \AA brightenings were likely photospheric $H\alpha$ -wing EBs, whereas more spread-out loop-like longer-duration brightenings were likely flaring arch filaments and small flares, bright in the transition-region diagnostics and probably bright at $H\alpha$ line center. Inspection of such flux-emergence AIA movies and of our high-resolution SST data suggests that distinction should be made between point-like (at SDO resolution) EBs and loop-like flaring arch filaments as different entities, respectively photospheric and upper-atmosphere. AIA's 1700 \AA shows fewer of the latter type and is therefore the best SDO diagnostic for EB studies. Figure 4 demonstrates that SDO's resolution is poor compared with the SST's, but the obvious AIA advantage is that it samples the stronger EBs in any Earth-side active region at any time.

Comment regarding EB fallacies: the low resolution of older data has led to claims of apparent co-spatiality of higher-atmosphere brightenings with EBs. Examples: coincidence with EBs was claimed for 6 out of 16 microflares by [93], but the example pair in their Figs. 4 and 5 has 8 arcsecond separation. The $H\alpha$ line-center brightening observed and modeled by [94] was not an EB. The $H\alpha \pm 0.35 \text{ \AA}$ feature claimed by [95] to be an EB at 1 MK doesn't look like an EB to us. The long-lived EB of [96] at the foot of an arch filament looks like a large MC. Similarly for the Ca II H bright points bordering the flaring arch filament in [97], much like the bright points of [93]. [6] reported one coincidence of X-ray brightening at an exceptionally bright EB but doubted frequent co-spatiality. We have aligned our new SST data with SDO/AIA image sequences and searched for but did not find any significant EB impact on the overlying transition region ($\text{He I } 304 \text{ \AA}$) and corona ($\text{Fe IX } 171 \text{ \AA}$) [10].

Comment regarding EB fads: most EB studies are based on observations in the $H\alpha$ wings and typically describe a single, a few, or at most some dozen EBs in a single active region during a short period. This type of study should exploit IRIS in the near future since EBs will be well visible in Mg II h \& k , as in Ca II H \& K . On the other hand, it seems time to exploit the AIA 1700 \AA database to study very many more with respect to occurrence patterns.

5. Ellerman bomb detection

In [9] EBs were identified and selected manually on the basis of their flame morphology in the SST $H\alpha$ -wing movies, meaning bright, narrow, tall, upright, flickering appearance in the limbward view at this unprecedented resolution. More formal detection criteria are formulated for two SST data sets in [10]. One of the requirements defining an EB kernel is 55% excess intensity in the $H\alpha$ wings over the spatial average of the active region, while setting a threshold of 5σ or higher above the mean seems a good counterpart to select EBs in AIA 1700 \AA images. Both thresholds are passed by the EBs in Fig. 4, whereas almost none of the bright $H\alpha$ -wing features in the movie sampled in Fig. 1 passed a 55% $H\alpha$ -wing excess threshold, nor a 5σ excess threshold in simultaneous 1600 \AA images from TRACE⁴.

⁴ Recently [60] claimed to detect 3570 EBs during 90 minutes around a small spot rather like the one in Fig. 1. Our application of the above threshold to the simultaneous SDO 1700 \AA images suggests that they mostly detected

In addition, small spatial extent is a discriminator, as already suggested by Ellerman: “On rarer occasions they [EBs] are superposed on bright reversals of $H\alpha$ over eruptive regions, but this is an uncommon occurrence, and the distinction is easily made between the two phenomena by the flickering of the “bomb” band compared to the $H\alpha$ reversal, due to the effect of seeing.” – as using scintillation to distinguish stars from planets. Small size, fast variation, large brightness, and appearing in a region with much flux emergence together become the recipe to locate EBs in AIA 1700 Å image sequences. We are presently refining such automated detection for multiple viewing angles [98].

6. Ellerman bomb radiation mechanism

In traditional one-dimensional stratification modeling along a vertical line of sight the emergent $H\alpha$ profile maps the variation of the source function with depth, with the outermost wings sampling the deepest layers [99]. Postulating a suited temperature perturbation with appropriate structure and motion to a standard model atmosphere can then explain any $H\alpha$ excess emission profile [100] [88], but not unambiguously; different models may produce similar $H\alpha$ profiles [91].

In the slanted perspective of Figs. 3 and 4 the EB flames appear as extended, dense, hot slabs that stick up from the network MCs into the otherwise $H\alpha$ -transparent upper photosphere, making cloud modeling more appropriate than one-dimensional plane-parallel modeling. The EB excess emission and its profile including its moustache extent are properties of such a slab, while the core absorption and Dopplershift patterns are properties of the overlying fibrils. Further away from line center the slab is optically thinner but not “deeper”.

We attribute the non-visibility of the EB slabs in neutral-metal lines to neutral-metal ionization in the hot EB flames, and similarly their transparency in the continuum to H^- ionization. Considerable ionization of neutral hydrogen is also likely, making cascade recombination the main producer of the EB $H\alpha$ photons. Even if the ionization occurs only briefly during a short reconnection event, $H\alpha$ will so shine in a longer-duration afterglow because hydrogen recombination balancing is slow in the aftermath [41] [42].

Following the suggestion of [101] we attribute the extended bright moustaches to subsequent thermal Thomson scattering of these photons, notwithstanding the small process crosssection, because the flames combine high temperature with very high (mid-photosphere) density. While the line-center peak of the EB brightness profile remains hidden by overlying fibrils, the wings may gain brightness at large thermal electron Dopplershift whenever a line-core photon meets an electron and is scattered our way. Since EBs are very optically thick at $H\alpha$ line center, being non-transparent already in the outer wings, we suggest that $H\alpha$ resonance scattering confines line-core photons in a random walk within the EB until they are Dopplershifted into a wing and escape. This scattering mechanism will produce similar moustaches for other chromospheric lines (principally Mg II h & k, Ca II H & K, and Ca II 8542 Å) if an EB similarly confines scattering line photons, which is likely unless these ions ionize too much. Obviously, numerical simulation with detailed spectral synthesis including non-monochromatic Thomson scattering may vindicate this moustache mechanism.

In this view large moustache extent happens *because* EBs are photospheric and makes them visible beyond the overlying fibrils in the spectrum. For $H\alpha$ such scattering occurs only within the flame, there being neither free electrons nor hydrogen atoms in the $n = 2$ level in the surrounding atmosphere, and so it remains local. Flame images taken in the outer $H\alpha$ wings therefore remain sharp, as demonstrated in Figs. 3 and 4. In Ca II H & K EBs get a diffuse halo from additional resonance scattering in the surrounding upper photosphere [90].

Comment regarding EB fallacies: Severny [49] [50], recognizing that the moustache extent cannot be explained by Stark broadening, invoked an EB scenario of nuclear explosion and pseudo-EBs of which the $H\alpha$ -wing brightness has nothing to do with MHD heating.

relativistic particle beams. This way of thinking became a school of thought in which flares and moustaches are regarded as similar phenomena, often mentioned together, in which the photosphere is hit from above by particle beams due to reconnection in the upper atmosphere. Such beams would then explain the lack of $H\alpha$ line-core brightening by passing through and not affecting the $H\alpha$ chromosphere. Linear line-core polarization attributed to the beam impact became the diagnostic for this notion [102] [103] [104] [105] [106] [107] [108] [109] [88] [110]. In our opinion these authors failed to recognize that EBs are photospheric and occur without anything happening overhead. We note that in the example of [102] the polarization is not cospatial with the moustache, and that the excess emission profiles of [103] have no dip at line center. We suspect that the measured line core polarizations stem from flaring arch filaments, possibly through the mechanism of [111].

7. Ellerman bomb occurrence

The SST samples in Fig. 4 include magnetograms that show examples of what we find to be characteristic behavior in these data. Small white opposite-polarity Stokes-V patches produce EB flames in the $H\alpha$ wing when colliding at relatively high speed with larger black patches, and then vanish. This is good evidence, similar to [90] but at higher resolution and with better statistics, that EBs mark strong-field cancelation and supports the notion that the bright EB flames are caused by photospheric reconnection [112] [113] [4] [80] [81] [114] [63] [9]. The gasdynamical instability proposed by [115] seems a less likely explanation since it does not have field emergence as necessary condition.

Strong opposite-polarity field emergence may happen with small-scale \cap loop shape in classical Ω emergence [116] or with additional \cup loop shape in serpentine emergence from the Parker instability [117] [118], with connecting arch filaments [119] accompanied by dipped fields and bald patches [3] [7] [8] [65] [120] [121] [114] [122] (see cartoons in [65] [122] [123]). In this picture chromospheric convergence of \cup loop sides is thought to give reconnection in the line-tied regime [80] [123], but the EBs in our SST data occur at colliding photospheric flows in the frozen-in regime (Fig. 4).

Comment regarding EB fads: serpentine patterning into opposite-polarity pairs of the MCs in the moat flow around decaying spots was already suggested by [14], but since EBs are emerging-flux phenomena it is tempting to assume serpentine emergence and \cup loop patterning. This scenario may well be valid, but convincing proof requires long-duration wide-field imaging spectroscopy with spectral, spatial, and temporal resolution at least comparable to our SST sequences. Obviously an IRIS topic. Photospheric feature tracking following [124] would be a good technique to analyze such data. Likewise, the notion of bi-directional anemone-jet flows with reconnection a few hundred km up is attractive but needs further verification.

8. Conclusion: Ellerman bomb usage

EBs are the most spectacular solar photosphere phenomenon. They seem especially informative as space-time markers of strong-field reconnection events in the photosphere, better than searching for bipolar cancelation in magnetograms. Comparison of the SST and HMI magnetograms in Fig. 4 illustrates the need for superhigh resolution and sensitivity in the latter approach and shows that even at the high SST quality one would not be able to identify reconnection events from magnetogram sequences alone. Larger Stokes sensitivity is desirable but longer integration would degrade the temporal and spatial resolution fatally. Thus, EB detection seems a better way to locate small-scale reconnection events in emerging flux regions. Since the larger and brighter EBs are also visible in 1700 Å images even at the AIA resolution, the AIA database permits monitoring active-region field re-configuration through EB identification in large data volumes [98]. EBs may so become useful photospheric telltales in studying chromospheric active-region field topology evolution and energy loading.

Acknowledgments

We thank R. Rezaei for informative discussions and the referee for valuable suggestions. RJR acknowledges that the late C. Zwaan often suggested EBs as research topic, and thanks the Leids Kerkhoven-Bosscha Fonds for travel support. We made much use of NASA's Astrophysics Data System Bibliographic Services. The macro to make the citations above link to ADS (at least in the arXiv preprint) was contributed by EDP Sciences.

References

- [1] Ellerman F 1917 *ApJ* **46** 298
- [2] Bray R J and Loughhead R E 1974 *The solar chromosphere* Chapman & Hall, London
- [3] Bernasconi P N, Rust D M, Georgoulis M K and Labonte B J 2002 *Solar Phys* **209** 119
- [4] Georgoulis M K, Rust D M, Bernasconi P N and Schmieder B 2002 *ApJ* **575** 506
- [5] Schmieder B, Pariat E, Aulanier G, Georgoulis M K, Rust D M and Bernasconi P N 2002 *Solar Variability: From Core to Outer Frontiers (ESA Special Publication 506)* ed Wilson A 911
- [6] Schmieder B, Rust D M, Georgoulis M K, Démoulin P and Bernasconi P N 2004 *ApJ* **601** 530
- [7] Pariat E, Aulanier G, Schmieder B, Georgoulis M K, Rust D M and Bernasconi P N 2004 *ApJ* **614** 1099
- [8] Pariat E, Aulanier G, Schmieder B, Georgoulis M K, Rust D M and Bernasconi P N 2006 *Adv Space Research* **38** 902
- [9] Watanabe H, Vissers G, Kitai R, Rouppe van der Voort L and Rutten R J 2011 *ApJ* **736** 71
- [10] Vissers G, Rouppe van der Voort L H M and Rutten R J 2013 *ApJ* submitted
- [11] Vitas N, Viticchiè B, Rutten R J and Vögler A 2009 *A&A* **499** 301
- [12] Sheeley Jr N R 1969 *Solar Phys* **9** 347
- [13] Vrabc D 1971 *Solar Magnetic Fields (IAU Symp 43)* ed Howard R 329
- [14] Harvey K and Harvey J 1973 *Solar Phys* **28** 61
- [15] Vrabc D 1974 *Chromospheric Fine Structure (IAU Symp 56)* ed Athay R G 201
- [16] Muller R and Mena B 1987 *Solar Phys* **112** 295
- [17] Hagenaar H J and Shine R A 2005 *ApJ* **635** 659
- [18] Spruit H C 1976 *Solar Phys* **50** 269
- [19] Spruit H C 1977 *Magnetic flux tubes and transport of heat in the convection zone of the Sun*. PhD Thesis Utrecht Univ
- [20] Spruit H C 1981 in *The Sun as a Star* ed Jordan S *NASA Special Publication* **450** 385
- [21] Deinzer W, Hensler G, Schüssler M and Weisshaar E 1984 *A&A* **139** 426
- [22] Knölker M, Schüssler M and Weisshaar E 1988 *A&A* **194** 257
- [23] Spruit H C, Schüssler M and Solanki S K 1991 *Filigree and flux tube physics in Solar Interior and Atmosphere* Univ Arizona Press 890
- [24] Solanki S K and Brigljevic V 1992 *A&A* **262** L29
- [25] Bünte M, Solanki S K and Steiner O 1993 *A&A* **268** 736
- [26] Solanki S K 1993 *Space Science Rev* **63** 1
- [27] Yelles Chaouche L, Solanki S K and Schüssler M 2009 *A&A* **504** 595
- [28] Berger T E, Rouppe van der Voort L H M, Löfdahl M G, Carlsson M, Fossum A, Hansteen V H, Marthinussen E, Title A and Scharmer G 2004 *A&A* **428** 613
- [29] Rouppe van der Voort L H M, Hansteen V H, Carlsson M, Fossum A, Marthinussen E, van Noort M J and Berger T E 2005 *A&A* **435** 327
- [30] Title A M and Berger T E 1996 *ApJ* **463** 797
- [31] Livingston W and Wallace L 1987 *ApJ* **314** 808
- [32] Livingston W, Wallace L, White O R and Giampapa M S 2007 *ApJ* **657** 1137
- [33] Leenaarts J, Rutten R J, Sütterlin P, Carlsson M and Uitenbroek H 2006 *A&A* **449** 1209
- [34] Leenaarts J, Rutten R J, Carlsson M and Uitenbroek H 2006 *A&A* **452** L15
- [35] Rutten R J 2012 *Roy Soc London Phil Trans Series A* **370** 3129
- [36] Schoolman S A 1972 *Solar Phys* **22** 344
- [37] Rutten R J and Uitenbroek H 2012 *A&A* **540** A86

- [38] Leenaarts J, Carlsson M and Rouppe van der Voort L 2012 *ApJ* **749** 136
- [39] Zirin H and Stein A 1972 *ApJ* **178** L85
- [40] Christopoulou E B, Georgakilas A A and Koutchmy S 2001 *A&A* **375** 617
- [41] Carlsson M and Stein R F 2002 *ApJ* **572** 626
- [42] Leenaarts J, Carlsson M, Hansteen V and Rutten R J 2007 *A&A* **473** 625
- [43] Zhang J, Solanki S K, Woch J and Wang J 2007 *A&A* **471** 1035
- [44] Kato Y, Steiner O, Steffen M and Suematsu Y 2011 *ApJ* **730** L24
- [45] Rutten R J, Leenaarts J, Rouppe van der Voort L H M, De Wijn A G, Carlsson M and Hansteen V 2011 *A&A* **531** A17
- [46] Bonet J A, Márquez I, Sánchez Almeida J, Cabello I and Domingo V 2008 *ApJ* **687** L131
- [47] Jess D B, McAteer R T J, Mathioudakis M, Keenan F P, Andic A and Bloomfield D S 2007 *A&A* **476** 971
- [48] De Wijn A G, Rutten R J, Haverkamp E M W P and Sütterlin P 2005 *A&A* **441** 1183
- [49] Severny A B 1956 *The Observatory* **76** 241
- [50] Severnyi A B 1957 *Soviet Astron* **1** 668
- [51] Bruzek A 1968 *Structure and Development of Solar Active Regions* (IAU Symp 35) ed Kiepenheuer K O 293
- [52] Turon P J and Léna P J 1970 *Solar Phys* **14** 112
- [53] Bruzek A 1972 *Solar Phys* **26** 94
- [54] Zachariadis T G, Alissandrakis C E and Banos G 1987 *Solar Phys* **108** 227
- [55] Stellmacher G and Wiehr E 1991 *A&A* **251** 675
- [56] Denker C, de Boer C R, Volkmer R and Kneer F 1995 *A&A* **296** 567
- [57] Denker C 1997 *A&A* **323** 599
- [58] Nindos A and Zirin H 1998 *Solar Phys* **182** 381
- [59] Georgakilas A A, Christopoulou E B and Koutchmy S 1999 *Magnetic Fields and Solar Processes* (ESA Special Publication 448) ed Wilson A and et al 279
- [60] Nelson C J, Doyle J G, Erdélyi R, Huang Z, Madjarska M S, Mathioudakis M, Mumford S J and Reardon K 2013 *Solar Phys* in press (*Preprint* 1301.1351)
- [61] Kurokawa H, Kawaguchi I, Funakoshi Y and Nakai Y 1982 *Solar Phys* **79** 77
- [62] Pariat E, Schmieder B, Berlicki A, Deng Y, Mein N, López Ariste A and Wang S 2007 *A&A* **473** 279
- [63] Hashimoto Y, Kitai R, Ichimoto K, Ueno S, Nagata S, Ishii T T, Hagino M, Komori H, Nishida K, Matsumoto T, Otsuji K, Nakamura T, Kawate T, Watanabe H and Shibata K 2010 *PASJ* **62** 879
- [64] Harvey J W 1963 *The Observatory* **83** 37
- [65] Watanabe H, Kitai R, Okamoto K, Nishida K, Kiyohara J, Ueno S, Hagino M, Ishii T T and Shibata K 2008 *ApJ* **684** 736
- [66] Gingerich O, Noyes R W, Kalkofen W and Cuny Y 1971 *Solar Phys* **18** 347
- [67] Vernazza J E, Avrett E H and Loeser R 1981 *ApJS* **45** 635
- [68] Fontenla J M, Avrett E H and Loeser R 1993 *ApJ* **406** 319
- [69] Avrett E H and Loeser R 2008 *ApJS* **175** 229
- [70] Leenaarts J, Rutten R J, Reardon K, Carlsson M and Hansteen V 2010 *ApJ* **709** 1362
- [71] Koval A N and Severny A B 1970 *Solar Phys* **11** 276
- [72] Beckers J M 1962 *Australian Journal of Physics* **15** 327
- [73] Dere K P, Schmieder B and Alissandrakis C E 1990 *A&A* **233** 207
- [74] Teriaca L, Curdt W and Solanki S K 2008 *A&A* **491** L5
- [75] Dara H C, Alissandrakis C E, Zachariadis T G and Georgakilas A A 1997 *A&A* **322** 653
- [76] Roy J R 1973 *Solar Phys* **28** 95
- [77] Roy J R and Leparskas H 1973 *Solar Phys* **30** 449
- [78] Carlqvist P 1979 *Solar Phys* **63** 353
- [79] Shibata K, Nishikawa T, Kitai R and Suematsu Y 1982 *Solar Phys* **77** 121
- [80] Isobe H, Tripathi D and Archontis V 2007 *ApJ* **657** L53
- [81] Matsumoto T, Kitai R, Shibata K, Otsuji K, Naruse T, Shiota D and Takasaki H 2008 *PASJ* **60** 95
- [82] Shimizu T, Martínez-Pillet V, Collados M, Ruiz-Cobo B, Centeno R, Beck C and Katsukawa Y 2007 *New Solar Physics with Solar-B Mission* (*Ast Soc Pacific Conf Series* 369) ed Shibata K, Nagata S and Sakurai T 113

- [83] Shibata K, Nakamura T, Matsumoto T, Otsuji K, Okamoto T J, Nishizuka N, Kawate T, Watanabe H, Nagata S, UeNo S, Kitai R, Nozawa S, Tsuneta S, Suematsu Y, Ichimoto K, Shimizu T, Katsukawa Y, Tarbell T D, Berger T E, Lites B W, Shine R A and Title A M 2007 *Science* **318** 1591
- [84] Morita S, Shibata K, Ueno S, Ichimoto K, Kitai R and Otsuji K I 2010 *PASJ* **62** 901
- [85] Nishizuka N, Nakamura T, Kawate T, Singh K A P and Shibata K 2011 *ApJ* **731** 43
- [86] Herlender M and Berlicki A 2011 *Central European Astrophys Bulletin* **35** 181
- [87] Qiu J, Ding M D, Wang H, Denker C and Goode P R 2000 *ApJ* **544** L157
- [88] Fang C, Tang Y H, Xu Z, Ding M D and Chen P F 2006 *ApJ* **643** 1325
- [89] Socas-Navarro H, Martínez Pillet V, Elmore D, Pietarila A, Lites B W and Manso Sainz R 2006 *Solar Phys* **235** 75
- [90] Matsumoto T, Kitai R, Shibata K, Nagata S, Otsuji K, Nakamura T, Watanabe H, Tsuneta S, Suematsu Y, Ichimoto K, Shimizu T, Katsukawa Y, Tarbell T D, Lites B W, Shine R A and Title A M 2008 *PASJ* **60** 577
- [91] Berlicki A, Heinzel P and Avrett E H 2010 *MemSAI* **81** 646
- [92] Fossum A and Carlsson M 2005 *ApJ* **625** 556
- [93] Kitai R and Muller R 1996 *Solar Phys* **165** 155
- [94] Guglielmino S L, Bellot Rubio L R, Zuccarello F, Aulanier G, Vargas Domínguez S and Kamio S 2010 *ApJ* **724** 1083
- [95] Madjarska M S, Doyle J G and De Pontieu B 2009 *ApJ* **701** 253
- [96] Herlender M and Berlicki A 2010 *Central European Astrophys Bulletin* **34** 65
- [97] Jess D B, Mathioudakis M, Browning P K, Crockett P J and Keenan F P 2010 *ApJ* **712** L111
- [98] Vissers G, Rouppe van der Voort L H M and Rutten R J 2013 in preparation
- [99] Rutten R J 2003 *Radiative Transfer in Stellar Atmospheres* Lecture Notes Utrecht University
- [100] Kitai R 1983 *Solar Phys* **87** 135
- [101] Engvold O and Maltby P 1968 *Mass Motions in Solar Flares and Related Phenomena* (Procs 9th Nobel Symp) ed Oehman Y 109
- [102] Babin A N and Koval A N 1985 *Solar Phys* **98** 159
- [103] Firstova N M 1986 *Solar Phys* **103** 11
- [104] Ding M D, Henoux J C and Fang C 1998 *A&A* **332** 761
- [105] Henoux J C, Fang C and Ding M D 1998 *A&A* **337** 294
- [106] Kazantsev S A, Firstova N M, Kashapova L K, Bulatov A V and Petrashen' A G 1998 *Russian Physics Journal* **41** 1258
- [107] Kosovichev A G and Zharkova V V 2001 *ApJ* **550** L105
- [108] Kashapova L K 2002 *Astron Reports* **46** 918
- [109] Zharkova V V and Kashapova L K 2005 *A&A* **431** 1075
- [110] Babin A N and Koval A N 2011 *Bulletin Crimean Astrophysical Observatory* **107** 36
- [111] Henoux J C, Chambe G, Heristchi D, Semel M, Woodgate B, Shine D and Beckers J 1983 *Solar Phys* **86** 115
- [112] Yokoyama T and Shibata K 1995 *Nature* **375** 42
- [113] Litvinenko Y E 1999 *ApJ* **515** 435
- [114] Archontis V and Hood A W 2009 *A&A* **508** 1469
- [115] Diver D A, Brown J C and Rust D M 1996 *Solar Phys* **168** 105
- [116] Zwaan C 1985 *Solar Phys* **100** 397
- [117] Parker E N 1966 *ApJ* **145** 811
- [118] Nozawa S, Shibata K, Matsumoto R, Sterling A C, Tajima T, Uchida Y, Ferrari A and Rosner R 1992 *ApJS* **78** 267
- [119] Strous L H and Zwaan C 1999 *ApJ* **527** 435
- [120] Cheung M C M, Schüssler M, Tarbell T D and Title A M 2008 *ApJ* **687** 1373
- [121] Pariat E, Masson S and Aulanier G 2009 *ApJ* **701** 1911
- [122] Pariat E, Masson S and Aulanier G 2012 *4th Hinode Science Meeting: Unsolved Problems and Recent Insights* (*Ast Soc Pacific Conf Series* 455) ed Bellot Rubio L, Reale F and Carlsson M 177
- [123] Pariat E, Schmieder B, Masson S and Aulanier G 2012 (*EAS Pub Series* 55) ed Faurobert M, Fang C and Corbard T 115
- [124] Strous L H, Scharmer G, Tarbell T D, Title A M and Zwaan C 1996 *A&A* **306** 947